Experimental Demonstration of the Control of Flexible Structures

David B. Schaechter* and Daniel B. Eldred†
Jet Propulsion Laboratory, California Institute of Technology, Pasadena, California

An experiment employing a pinned-free flexible beam has been constructed to demonstrate active shape control, active dynamic control, adaptive control, various control law design approaches, and associated hardware requirements and mechanization difficulties in connection with flexible structures. This paper describes the analytical work performed in support of the facility development, the final design specifications, the control law synthesis, and the experimental results.

Nomenclature

C = control feedback gain
EI = beam stiffness
F = finite element force vector
f = distributed force
g = gravitational acceleration
K = finite element stiffness matrix
K = Kalman gain
ℓ = beam length
M = finite element mass matrix
T = sample period
t = time
u = control force vector
x = finite element displacement vector
x = independent spatial variable
x = system state vector
y = beam displacement
y_d = desired shape function
z = measurement vector
Φ = state transition matrix
ρ = linear density of beam

Introduction

ONE of the most intensely studied subjects in control system design has been the control of large flexible space structures. Industry, government, and universities have combined efforts to produce numerous approaches to surmount the problems associated with the control of this new type of space vehicle. In some instances, the validation of these new control approaches has been theoretical in nature; in other cases, computer simulations have been used to demonstrate the feasibility of these control approaches on specific applications. Even more recently, experimental facilities such as the one described in this paper have been constructed to demonstrate, in hardware, the control of flexible structures.[1]

The Large Space Structure Technology (LSST) Flexible Beam Experiment was constructed to demonstrate several facets of the control of large flexible space structures. The desired features of this experiment were to demonstrate 1) active shape control, 2) active dynamic control, 3) various control law design approaches, 4) adaptive control, and 5) microprocessor control capability.

Received May 9, 1984.

*Member of Technical Staff; currently, Research Scientist, Lockheed Missiles and Space Company, Palo Alto, Calif. Member AIAA.

†Member of Technical Staff. Member AIAA.

This paper describes much of the work performed in support of the facility development, the final design specifications, control law synthesis, and some experimental results.

Experiment Hardware

Configuration

A flexible beam was chosen for this experiment because it is a simple, continuous structure with many of the dynamic characteristics that are representative of general large space structures, including infinitely many vibration modes, a rigid-body mode, and many low-frequency vibration modes. The beam configuration allows for testing shape control, vibration control, and adaptive control laws with a single experimental apparatus.

A photograph of the beam and its support structure (tower) is shown in Fig. 1. The tower is constructed of aluminum

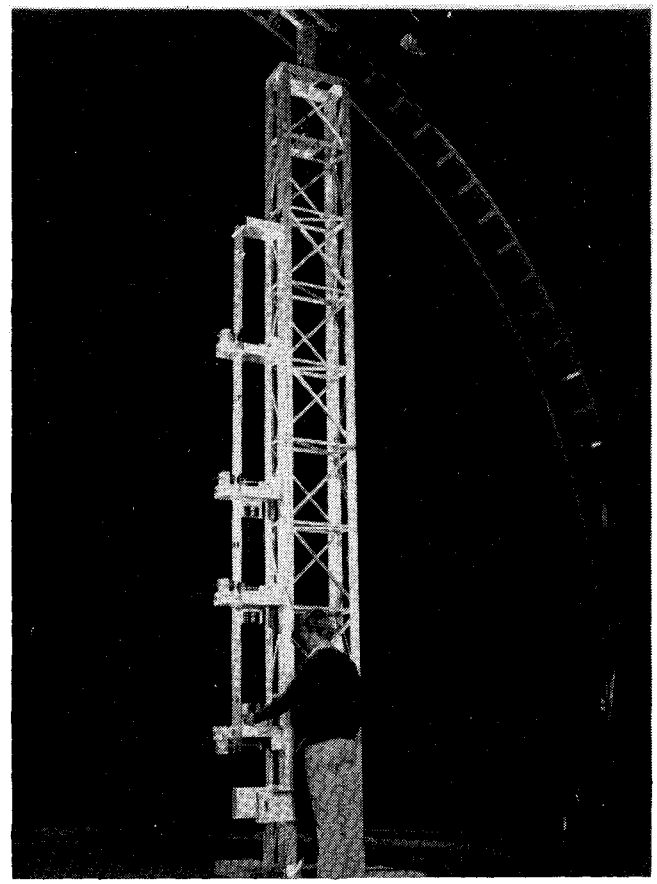

Fig. 1 The flexible beam and its support structure.

Table 1 Tower resonances

Frequency (Hz)	Mode	Direction
6	Cantilever	Compliant
10	Cantilever	Stiff
27	Pinned-free	Compliant
35	Pinned-free	Stiff
45	Free-free	Compliant
63	Free-free	Stiff

Table 2 Natural frequencies, Hz

n	Analytical	10 Divisions	20 Divisions	Measurements
0	0.301	0.308	0.308	~0.34
1	0.728	0.755	0.755	0.75
2	1.27	1.38	1.38	1.37
3	1.98	2.21	2.21	2.15
4	2.92	3.25	3.24	3.16
5	4.08	4.51	4.47	4.38
6	5.49	6.00	5.93	
7	7.13	7.76	7.62	
8	9.03	9.79	9.55	
9	11.16	12.04	11.73	
10	13.54	15.92	14.15	

angles and is 20 ft high, 2 ft deep in the stiff direction, and 1 ft deep in the compliant direction. The weight of the tower is 200 lb. With the sensor/actuator mounting brackets (Fig. 2), beam, sensors, actuators, and electronics, the total weight is about 300 lb.

Shake tests were performed on the tower to determine its resonant frequencies and whether they might interact with those of the flexible beam. The results are given in order of increasing frequency in Table 1.

For the hanging beam, only the natural frequencies in the stiff direction are of interest because there is very little coupling between motions in perpendicular directions. Since the tower resonant frequencies corresponding to the stiff direction are much higher than the first several natural beam frequencies (see Table), it was concluded that the support tower interaction with the beam motion would be negligible.

A schematic drawing of the sensor/actuator mounting bracket is shown in Fig. 2. Either the sensor, or actuator, or both may be mounted on a single bracket, and the brackets may be mounted at any of the stations located at 6-in. intervals along the beam.

Sensors

Eddy current position sensors made by Kaman Science Corporation were selected for the primary sensing system for the hanging beam experiments. Each unit has an accuracy of 0.001 in. over a ±1 in. range, with a 30 Hz bandwidth, according to the manufacturer's specifications. The sensor support bracket was made from lucite as part of the effort to locate all metal objects (except the beam) sufficiently far from the sensor to avoid undesirable interaction.

Actuators

The maximum actuation force and bandwidth are dictated by the requirements for dynamic control, since static shape control requires far less bandwidth and force. The actuators selected were brushless dc torque motors manufactured by Aeroflex Laboratories, Inc. With a 3-in. moment arm, and the appropriate mechanical linkages, each actuator has the capability of applying 5 oz of force to the beam for a maximum 1 A input with a bandwidth of 30 Hz, according to the manufacturer's specifications.

The mechanical linkage and the rotor of the brushless dc motor can be seen in Fig. 2. The mechanical linkages were

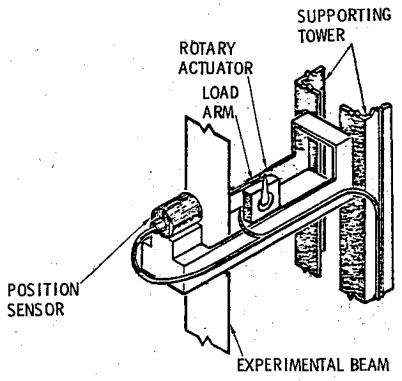

Fig. 2 Closeup of the sensor/actuator mounting bracket.

designed with miniature ball bearings at the motor end and flex hinges at both ends to minimize torsional interactions with the beam, since torsional motion was neither observed nor controlled in any of the experiments.

Display

For display purposes three retroreflecting mirrors were attached to the beam. A laser source mounted across the room from the flexible beam delivers three equal intensity laser beams, and these in turn are reflected by these mirrors onto a screen. The positions where the three laser beams impinge on this screen provide a visual display of the rotation of the corresponding sections of the beam. This display is used for static shape control demonstration.

Microcomputer

The purpose of the microcomputer is to sample the data from the sensors, pass these sampled data through a digital filter, and send appropriate commands to the actuators. The microcomputer chosen for the control function is the SYM-1 by Synertek System Corporation. It is based on a 6502 microprocessor operating a 1 MHz clock speed. The onboard memory capacity is 4K of random access memory (RAM) and 6K of read-only memory (ROM). A dynamic RAM board manufactured by The Computerist provides 16K of additional volatile memory, sockets for up to 16K of read-only memory, an erasable, read-only memory (EPROM) programmer, and two general-purpose timer/ports.

To take advantage of the many S-100 products available, and since the SYM-1 is not directly compatible with the S-100 bus (the S-100, IEEE-696 bus is an industry standard for interfacing microcomputer circuit boards), a KIMSI Interface/Motherboard by Forethought Products was added. Specifically, the digital-to-analog converters and the arithmetic processor are S-100 circuit boards.

Arithmetic Processor

A recent addition to the experiment is an AMD 9511 arithmetic processor by Advanced Micro Devices mounted on a custom-made circuit board. Previously, computations were performed by the 6502 microprocessor in software. The 9511 is a stack-oriented device which performs four-byte floating point multiplications in about 50 μs. Combined with driver software to control it, an operation (roughly one multiplication plus one addition) can be performed approximately four times as rapidly with the arithmetic processor as with the 6502, while at the same time internal computations are more accurate because four bytes, instead of two, are used to represent numbers.

Software Development

Highly interactive software has been developed to facilitate the implementation of a variety of control laws. The interactive loops are coded in BASIC, while the speed-critical

real-time control loops are coded directly in assembly language. Data are passed automatically from BASIC to the machine language subroutines.

An interpreter has been written to simplify the construction of a control algorithm from the machine language building blocks. The stack-oriented interpreter allows matrix manipulations to be performed in a reverse-Polish calculator-like style. For example, 1 2 * causes matrix 1 to be multiplied by matrix 2. Dimensions are handled automatically. Since the interpreter is written is machine code, the time penalty associated with its use is minimal. The instruction set of the interpreter is summarized in Table 3.

Shape control laws, dynamic control laws, and adaptive control laws all can be implemented with the simplified format required by the matrix interpreter and considerable time is saved when implementing new and different control laws with the interpreter.

Timing

Due to the limitation imposed by the sampling theorem (i.e., sample two or more times per cycle), the computation time is an important parameter for control design. Assuming the following general format for the digital filter,

$$x_{k+1} = \Phi x_k + K z_k, \qquad u_k = C x_k$$

one can determine the computation time by means of the following formula:

$$T \approx (n^2 + np + nm)\, T_* + nT_+ + pT_{\text{in}} + mT_{\text{out}}$$

where n is the number of states, p the number of sensors, m the number of actuators. T_*, T_+, T_{in}, T_{out} are, respectively, average times for multiplication plus addition, addition, sampling a sensor, and outputting a control; these include the times needed to perform an actual computation plus the time required for moving data around, setting up do-loop counters, and other overhead.

Table 4 gives the time required by either the microprocessor or the arithmetic processor for performing arithmetic. The execution times for sensor input and control output were determined from an instruction count. Those for multiplication and addition were obtained by recording the time required to multiply or add large matrices with a stopwatch and then dividing by the number of operations. The fact that the 9511 internal stack was used for storing intermediate results when multiplying matrices accounts for T_* being smaller than T_+.

Experience shows that somewhere in the vicinity of 15-20 (or more) samples per period are necessary for satisfactory performance of a Kalman filter/optimal controller. This condition is met by the 6502 microprocessor using a six-state (i.e., three normal modes) estimator/controller or by an eight-state estimator/controller using the 9511 arithmetic processor. Thus, while its extra speed is important for implementing adaptive control, the arithmetic processor yields only modest increases in the complexity of control algorithms which can be implemented using it. Its major contribution to the experiment is to allow calculations in four-byte floating point format, instead of the two-byte fixed format used by the 6502, in which case numbers have to be carefully scaled to avoid overflow and truncation errors.

D/A and A/D Conversions

Three of the four 12-bit Vector-Graphic digital-to-analog (D/A) converters are dedicated to outputting proper voltages to the actuators under microprocessor control. The fourth is used to sample up to eight sensor outputs. Currently four sensors are available. Sampling of the sensor outputs is accomplished by a successive binary comparison method in software.

Other Microcomputer Features

An assembler/editor is provided for developing machine language programs. An advanced debugging monitor is used for testing them. Microsoft BASIC is used for programming tasks which are not time-critical, such as converting matrix data to the format required by the arithmetic processor and poking them into memory. A keyboard and a video display combine to provide terminal functions, and an inexpensive audio cassette recorder is used to store programs.

Static and Dynamic Analysis

A static model of the hanging, pinned-free beam is required for static shape control,[2] and a dynamic model is required for dynamic control system design. For complex structures, a general-purpose finite element program such as NASTRAN[3] is generally required for obtaining the natural frequencies and mode shapes. However, the relative simplicity of the experimental beam permits one to employ an approximate analytical analysis and to develop a very precise finite element model which includes an exact stiffness matrix for deriving static shape control feedback gains.

Table 3 Interpreter instructions

Instruction	No. of Operands	Functions
PLUS	—	Adds two matrices
TIMES	—	Multiplies two matrices
RECALL	1	Recalls a matrix
STORE	1	Stores a matrix
INPUT	—	Inputs a measurement vector
INPUT 1	1	Inputs one sensor
OUTPUT	—	Outputs a control vector
OUTPUT 1	1	Outputs one control
ROTATE	—	Rotates four-element stack
PUSH	—	Duplicates top of stack entry
POP	—	Eliminates top of stack entry
EXCHANGE	—	Exchange top of stack entries
SETTIME	2	Sets loop timer clock
WAIT	—	Waits until time runs out
BREAK	—	Checks for break key and return to BASIC
JUMP	1	Jumps to another location
STOP	—	Stops (for debugging)

Table 4 Control loop timing

	Microprocessor	
	6502, ms	9511, ms
T_{in}	0.64	0.67
T_{out}	0.06	0.37
T_*	0.99	0.24
T_+	0.08	0.27

Table 5 Beam characteristics

Material	Stainless steel
Length, ℓ, in.	149-7/8
Width, in.	6
Thickness, in.	1/32
Flexural rigidity, EI, lb-in.^{2}	424.3
Weight, lb	8.05

The partial differential equation describing the beam motion is

$$\rho\frac{\partial^2 y}{\partial t^2}+EI\frac{\partial^4 y}{\partial x^4}-\rho g\frac{\partial}{\partial x}\left[(\ell-x)\frac{\partial y}{\partial x}\right]=f$$

The first term is the inertia force of the beam, the second term is due to beam stiffness, the variable tension along the length of the beam due to gravity is reflected in the third term, and f is the externally applied force. The values of the beam parameters were determined experimentally and are summarized in Table 5.

An effort to find exact analytical solutions of the beam dynamical equation proved fruitless (the solution of the time-independent equation involves Bessel functions of fractional order), so an approximate analytical model was developed for use in the early stages of the project. It can be shown that the squares of the exact eigenvalues are approximately the sum of the squares of the corresponding frequencies of the hanging chain and the pinned-free beam (both of which can be determined analytically), with the largest error occurring when these two frequencies are nearly equal. This result was obtained by assuming that the mode shapes for both simple cases are identical. The analytically determined mode frequencies are presented in Table 2.

Initial dynamic control experiments using these frequencies and the pinned-free beam mode shapes were satisfactory, but the need for a much more accurate model prompted the development of a discretized, finite element model. The beam was divided into segments, and the displacements and slopes at the ends of the segments were employed as coordinates. The usual course for defining mass and stiffness matrices of each element involves choosing some interpolation or spline function for the displacement as a function of distance; in this case, truncated infinite series solutions of the static differential equation were used as the interpolation functions. The advantage of using series solutions in this manner is that the resulting elements of the overall stiffness matrix, which give the force/deflection influence coefficients, are exact (within machine precision), and that fewer elements are required to accurately determine normal modes than if simpler spline functions were used.

The mass and stiffness matrices are assembled to create overall mass and stiffness matrices for the system. The differential equation for dynamic motion is thereby replaced by a matrix eigenproblem, and arbitrary accuracy can be obtained by considering smaller divisions of the beam. The dynamic equation of motion in matrix form becomes

$$M\ddot{x}+Kx=F$$

where F consists of the forces and torques applied at node points. In practice, a 20-element model has proved to be satisfactory for both static and dynamic analysis.

A comparison of the first 10 beam frequencies as obtained via the aforementioned approximate analytical method, the finite element method, and direct measurements are displayed in Table 2. The experimental values were obtained from a Fourier analysis of the impulse response of the beam. Excellent agreement is obtained, at least for the first four or five modes, indicating an accurate model. The first four mode shapes obtained from the finite element model are shown in Fig. 3.

Static Shape Control

The main application of static shape control is to control the surface of an antenna dish actively to maintain an optimal shape for signal focusing. More generally, static shape control may be required in any application where the precise undeformed geometry of a structure is to be maintained. The common features of the shape control problem treated here are: 1) the structure can be represented accurately by a continuous model, 2) the desired shape is specified a priori and may consist of a continuous shape, a set of discrete displacements, or a combination of the two, and 3) a finite number of discrete sensors and actuators are distributed about the structure for estimation and control, respectively.

This section presents the results of two different implementations of static shape control in the flexible beam experiment. In the first approach, a desired shape which is compatible with the beam's geometric boundary conditions, is specified. Some or all of the four position sensors are used for estimating the beam displacement, and the actuator forces required to produce the desired shape are computed and output to the three actuators. Some iteration in the process is required to remove the effects of bias.

In the other approach, the rotation of the beam is controlled rather than the displacement. In this case, the desired shape is specified as a set of discrete rotations. Since the eddy current position sensors cannot measure rotation, a scheme using a laser, in which the laser light is reflected from mirrors attached to the beam, was devised (Fig. 4). The experimental results proved to be very sensitive to modeling errors, so the model was improved using a parameter identification algorithm.

The mathematical theory for static shape control and estimation using quadratic performance indices is treated extensively in Ref. 4. A Green's function approach is used, the result being an analytical solution in which the continuous nature of the structure, the discrete nature of the sensors and actuators, and the boundary conditions, are handled together naturally. The existence of the analytical solution makes it possible to use the full-order model rather than a truncated model for control system design; however, for practical reasons, a finite element model, rather than partial differential equations, is used for the numerical computations.

The Green's function, required for calculation of the optimal control and estimation laws, can be obtained in two different ways. One method is to develop an expansion in terms of the system's eigenvectors. Since the series converges rapidly and, therefore, can be truncated without much loss of accuracy, this method is useful for approximating the Green's function of a very large order system if the low-order eigenvectors are available. The other method is to invert the finite element stiffness matrix to obtain the compliance matrix. An element of the compliance matrix can be found by computing the displacement occurring at one point of the

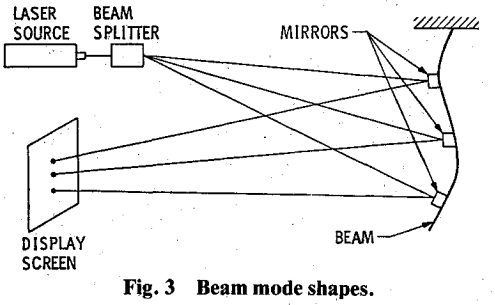

Fig. 3 Beam mode shapes.

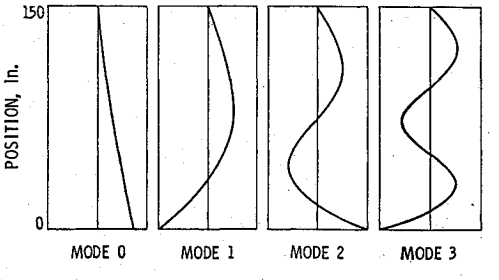

Fig. 4 Laser beam display.

structure when a unit force is applied at another point; i.e., the Green's function evaluated at these two points. This method of calculating the Green's function was used for the shape control experiments described below.

Two desired shapes $y_d(x)$ were chosen for demonstration of shape control of displacement:

$$\text{Shape I} \quad y_d(x) = \frac{1}{2}\left(\frac{2x}{\ell} - \frac{x^2}{\ell^2}\right)$$

$$\text{Shape II} \quad y_d(x) = \frac{1}{2}\left(\frac{4x}{\ell} - \frac{4x^2}{\ell^2}\right)$$

Shape I consists of a parabola with its vertex located at the bottom end of the beam, and Shape II is a parabola which is symmetric about the middle of the beam. See Fig. 5.

Optimal estimates were obtained from the four position sensors, and optimal controls were applied by three position actuators.

The continuous displacements resulting from static shape control are shown in Fig. 5 for the two shape functions chosen. The curves labeled "open loop" give the beam deflection resulting from open-loop control; that is, the control gains are calculated a priori, a shape estimate is obtained, the shape error is determined, and a single set of controls is output to remove the error. The curves labeled "closed loop" are the result of using feedback to further improve the controlled shape; that is, a shape estimate is obtained, the shape error is determined, and a new control is output to correct this error. The process is repeated until no further improvement in shape is observed (usually about three iterations).

The rms shape error as a function of the number of sensors used in the control loop is given in Fig. 6. In the case that fewer than four sensors were used, only the bottom most ones were employed. These results show that the addition of more than one or two sensors to the control loop does not contribute very much to an improvement in performance. This is because the beam model is so good that knowledge of its deflection at any one point is sufficient information to determine the deflection over its entire length. The implication is that few sensors are required if the system model is good, and more are required for feedback if modeling errors exist.

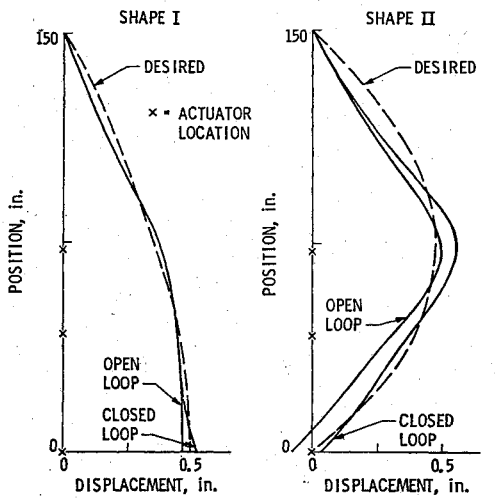

Fig. 5 Open- and closed-loop shape control.

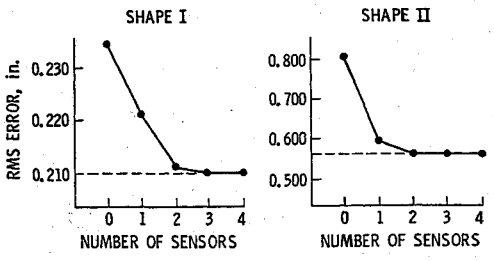

Fig. 6 Effect of sensors on control performance.

Initial difficulty in obtaining acceptable shape control performance on the beam experiment (attributed, in part, to hysteresis torque in the actuators) had to be overcome by executing static shape control recursively in a manner analogous to a Kalman filter. The resulting feedback control consists of the following sequence of events:

1) Sample the position sensors.

2) Estimate the beam deflection using these measurements, the known control outputs, and their respective uncertainties.

3) Compute the optimal control based on the difference between estimated and desired shapes.

4) Output the optimal control.

5) Go to the first step once beam motions have damped out.

The following qualitative observations were made once the algorithm was implemented:

1) The theoretically optimal shape is not achieved with one control iteration.

2) The shape of the beam converges rapidly (after about two or three iterations of the control loop) to some limit.

3) The limiting shape is generally quite close to the theoretically optimal shape, depending on how many sensors are used in the control loop.

The demonstration of shape control of rotation involves focusing the three reflected laser beams to desired positions, which are linearly related to the rotations of the beam at the points where the mirrors are mounted. This type of shape control requires a slight modification of the algorithms in Ref. 4. Instead of the Green's function, the spatial derivative of the Green's function is required. If the eigenvector expansion is used to determine the Green's function, then the derivatives must be approximated using a finite difference scheme; however, inversion of the finite element stiffness matrix yields the derivatives (at discrete points) directly.

Difficulties in obtaining satisfactory results for shape control of rotation were traced to extreme sensitivities of results to model errors. Model identification was required to obtain satisfactory performance. Model identification of a static system for the purpose of shape control is simple both conceptually and mathematically. The object is to find a transfer matrix which most closely fits a set of input-output pairs, according to some criterion. The result, a matrix consisting of influence coefficients evaluated at discrete points, can be used in the control loop for greater accuracy and improved convergence of the shape control algorithm.

The performance criterion used in this case consisted of the trace of a quadratic function which favored the a priori model for few measurements, and favored the observed measurements if many data were available. The solution procedure leads to a linear matrix equation, which can be solved by the method of Bartels and Stewart.[5]

The approach works well as indicated by the following representative example. The initial positions of the three reflected laser beams were (0.0, 0.0, 0.0) on the display screen. The desired positions were chosen arbitrarily to be (1.0, 0.0, −1.0) in.

After one iteration of the control loop, the laser positions were (1.0, −0.2, −1.1) in. After two iterations, the positions were stable at (1.1, 0.0, −0.9) in. In each iteration, the four position sensors were used to estimate the beam's displacement, and the beam model in turn was used to estimate the rotation. Since the resolution of the reflected laser is about 0.2 in., the shape control of rotation is seen to work very effectively.

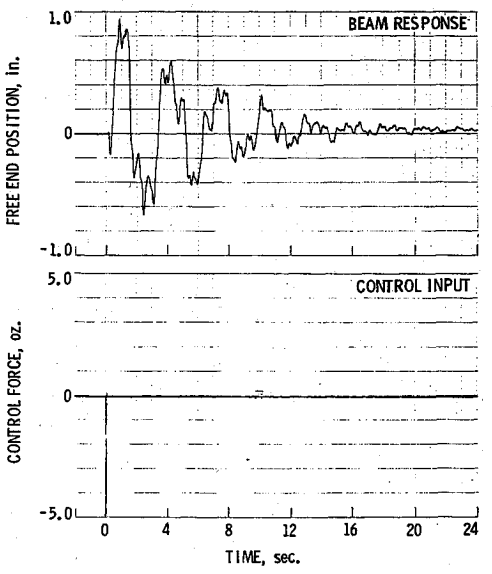

Fig. 7 Impulse response at free end of flexible beam.

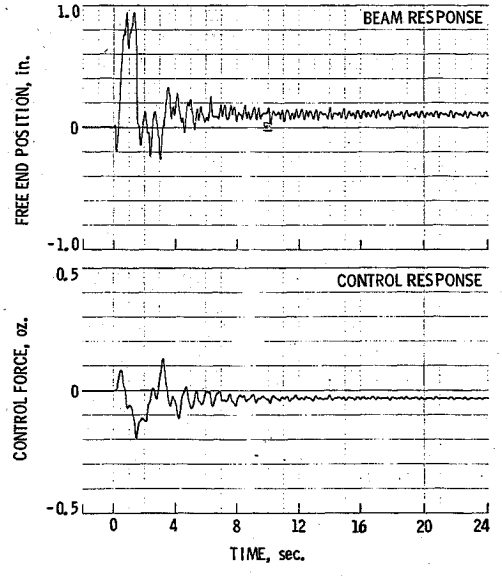

Fig. 8 Kalman filter/optimal control.

Dynamic Control

The Space Shuttle has made possible the deployment of larger and more complex space structures, such as antennas, platforms, and solar arrays. Such structures are very lightly damped and, therefore, may require active vibration suppression to maintain quiet operation and structural integrity.

Two distinct approaches to control the vibrations of the JPL flexible beam have been tested. The first approach is a well understood modal control design. The design process begins with a (truncated) modal model of the dynamic system. Using an optimal control design approach[1,6] an estimator/controller was implemented using the three lowest frequency modes of the system as the system model. It was anticipated that spillover effects would limit the performance achievable with this approach.

A second control system design approach was based upon a continuum model of the beam. The problem of control system design for distributed parameter systems was analyzed with the use of partial differential equations of motion.[7] The results of this analysis showed, in general, that, using spatially continuous sensors and actuators, it is possible to obtain the solution of the optimal control problem. This solution can be divided into two distinct control regimes: 1) the control of the low-frequency modes where local control is optimal, and 2) the stabilization of the high-frequency modes where Green's function-related feedback is optimal.

In both cases, since it is assumed in the analysis that spatially continuous sensors and actuators are available, no state estimation is required. In reality, only the spatially discrete analogs of these devices will be used. In this latter (more realistic) case, either a state estimator will be required to fill in the continuous state between the discrete sensors, or approximations to the control law must be made. In this example, the approximate control laws were implemented without the use of a state estimator.

As a point for future reference, Fig. 7 shows the open-loop response of the flexible beam. A force impulse was applied to the free end of the beam, and the resulting motion of the beam at the free end is plotted. It can be seen that many lightly damped modes are excited by the force impulse. The open-loop modal damping, primarily due to bearing friction and atmospheric drag, has been estimated, using maximum likelihood parameter estimation, to be about 3.0% of critical damping for most modes.

An optimal estimator/control design based on a modal model was the first approach used to actively damp vibrations of the beam. The six states included in the model used for controlling design were the amplitudes and amplitude rates of the three lowest frequency modes. Only the single position sensor at the free end of the beam was used for reconstructing the state estimates. In addition, only the single force actuator at the free end of the beam was used to control the beam. The sample time was 30 ms.

The results of using this controller are shown in Fig. 8. As can be seen, the resulting closed-loop system response damps out much more rapidly than the open-loop system response. In fact, the damping ratio achieved in the first mode is approximately 40% of critical damping. Residual oscillations are due to the unmodeled 2.2 Hz mode. This particular Kalman filter/optimal control design has the best performance of any tried to date. Attempts to improve the closed-loop response by decreasing the cost of the control in the performance index resulted in destabilization of the 2.2 Hz mode. Instability of unmodeled modes (control "spillover") is a common problem with control implementations and depends on many factors, including: sensor/actuator number and locations, inherent damping of the system, spectral distribution of natural frequencies, and the performance required of the control system.

The next control design approach is based upon the continuum structural model. This approach leads to disjoint actions taken by colocated sensor/actuator pairs, i.e., there is no communication between the various controllers on the flexible beam. As many as three such pairs can be implemented.

In order to control the flexible beam with the existing control hardware, both position and rate information must be included in the control law. Since only position sensors are used, the rate information must be derived.

A Kalman filter, or, in general, any observer, would combine the sensor measurements with a mathematical model in order to obtain smoothed position and rate estimates that are, in some sense, consistent with the model and the measurements. No state estimator was used in this distributed parameter system controller, therefore, in order to obtain the rate information, the position sensor outputs were differentiated to provide the local rate information. This is the purpose of the digital filter.

As might be expected, this type of controller is quite insensitive to modeling errors since no explicit use of the model is made in the implementation of the control system. Figures 9 and 10 show these results. Excellent vibration suppression is achieved in both cases with very little spillover into the higher

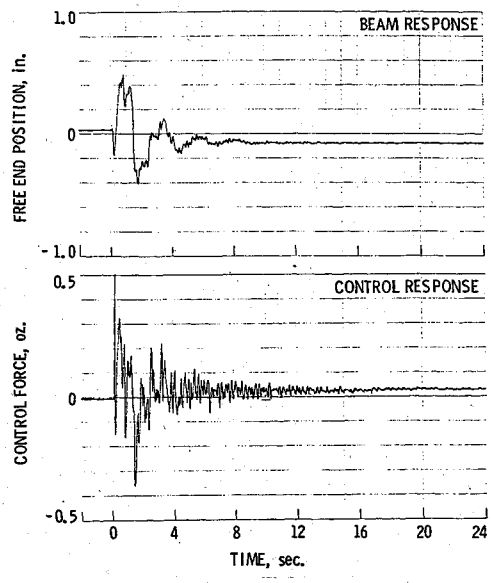

Fig. 9 Closed-loop response (one loop) of distributed control.

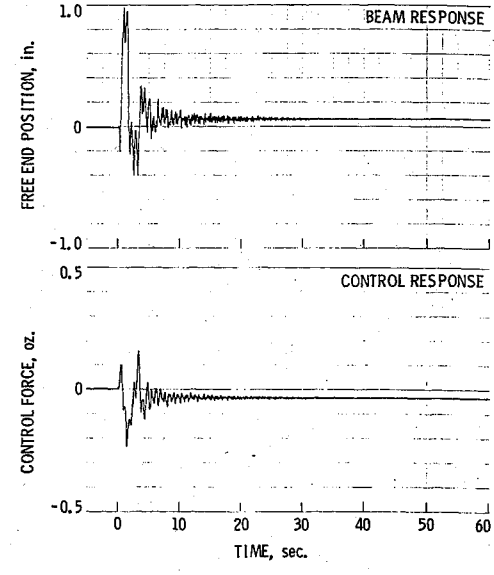

Fig. 11 Adaptive control/Kalman filter with correct model.

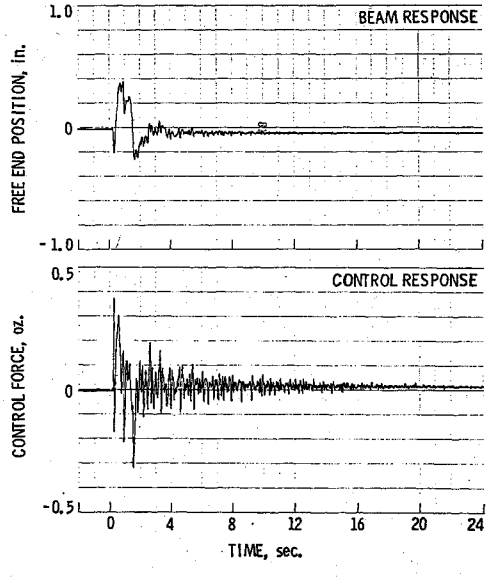

Fig. 10 Closed-loop response (three loops) of distributed control.

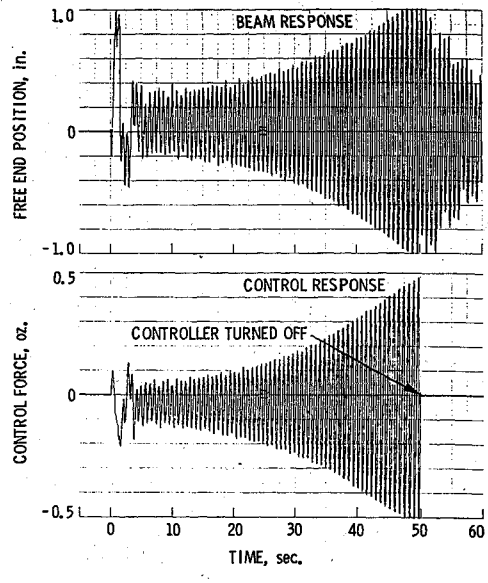

Fig. 12 Kalman filter/optimal control with model error.

frequencies. Due to the encouraging results obtained here, additional theoretical work on the control of distributed parameter systems is being performed.

Adaptive Control

Adaptive control techniques are being studied for their future application to the control of large space structures, where uncertain or changing parameters may destabilize closed-loop systems based upon standard control system designs.[8] The approach used in this section employs an extended Kalman filter in which the state vector is augmented with the parameters. The associated Ricatti equation is linearized about the case of exactly known parameters. If one assumes that parameter variations occur slowly, the filter complexity is reduced further.[9] Simulations on a two-degree-of-freedom oscillator demonstrated the parameter-tracking capability of this filter and paved the way for implementation of the JPL flexible beam.

A seven-state (six states for the first three modes, plus one additional state for the frequency of the third mode) adaptive filter/controller using only one sensor and one actuator (at the lower end of the beam) was developed for experimental testing.

Figures 11-14 compare the effects of using the Kalman filter/optimal control with the results of employing the adaptive estimator/optimal control. Each of these figures consists of the displacement of the beam due to an impulse at its lower end and the control force exerted. In one case, the assumed model is the correct model, and in the other case, the third eigenvalue was intentionally made 20% too large to reflect an uncertain model. A discussion of each figure is included.

In Fig. 11 the Kalman filter was replaced by an adaptive filter which estimates the third modal frequency in addition to the state. Since the initial model was exact, the beam response is virtually identical to the Kalman filter/optimal control response shown in Fig. 8.

In Fig. 12 the initial value for the third eigenvalue was set 20% too large. The Kalman filter/optimal control design cannot cope with the erroneous model and the system goes unstable.

In Fig. 13 the initial value of the third eigenvalue again was 20% too large. Unlike the Kalman filter/optimal control in

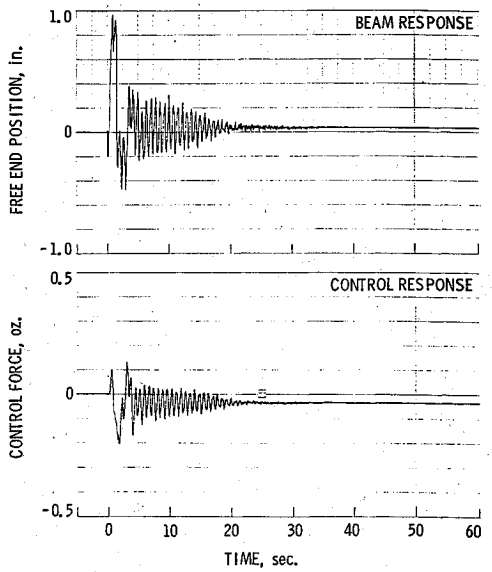

Fig. 13 Adaptive filter/optimal control with model error.

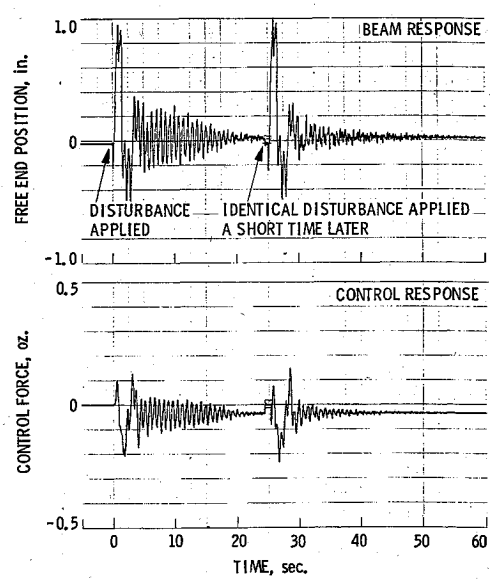

Fig. 14 Memory of adaptive filter.

Fig. 12, which was unstable, the adaptive filter effectively damps the system after an initial identification period.

Finally, Fig. 14 demonstrates the memory of the adaptive filter. Once the model has been identified correctly during the response to the first impulse, the response to the second impulse is improved greatly. The second impulse response is virtually identical to the response obtained by using the correct model initially.

Although in theory the extended Kalman filter is quite difficult to implement in real time, these results have shown that suitable approximations can make implementation tractable, while at the same time yielding good results. Of course, the virtues of adaptive estimators/controllers must be weighed against their disadvantages. More computation time is required, careful choice of feedback gains is necessary for stability, and care must be taken to avoid long-term instabilities. Nonetheless, there are few alternatives to using adaptive estimation/control if the system is evolving in time or the model is inaccurate, and these results demonstrate the viability of one type of adaptive estimation/control algorithm.

Summary

This flexible beam experiment is one of the first laboratory facilities constructed to demonstrate solutions to a diverse set of large structure control problems. Excellent results have been obtained thus far in shape control, modal control, distributed control, and adaptive control. The requirement of getting control systems to operate successfully on a large space structure-like system played a significant role in motivating the theoretical development of new control system approaches. At the same time, this requirement constrained the control design to be physically realizable in available hardware. Unmodeled torsional modes, sensor and actuator nonlinearities, computational delays, reversed signs, etc., are only a few of the difficulties encountered in trying to develop this facility. After these difficulties were overcome, the final product was a highly interactive facility for producing experimental results in the control of large structures.

Acknowledgments

Any development such as this requires a team effort. Steve Gunter, George Hotz, Ed Kan, Mark Nelson, Gary Parker, Jeff Schroeder, and Eldred Tubbs all deserve recognition as being a vital part of this team.

The research described in this paper was performed by the Jet Propulsion Laboratory, California Institute of Technology, under contract with the National Aeronautics and Space Administration.

References

[1]Schaechter, D. B., "Hardware Demonstration of Flexible Beam Control," *Journal of Guidance, Control and Dynamics,* Vol. 5, Jan./Feb. 1982, pp. 48-53.

[2]Eldred, D. B. and Schaechter, D. B., "Experimental Demonstration of Static Shape Control," *Journal of Guidance, Control and Dynamics,* Vol. 6, May/June 1983, pp. 188-192.

[3]Schaeffer, H. G., *MSC/NASTRAN Primer, Static and Normal Modes Analysis,* Wallace Press, Inc., Milford, N.H., Jan. 1982.

[4]Weeks, C. J., *Shape Determination and Control for Large Space Structures,* Jet Propulsion Laboratory, Pasadena, Calif., Pub. 81-71, Oct. 1981.

[5]Bartels, R. H. and Stewart, G. W., "Solution of the Matrix Equation $AX+XB=C$," *Communications of the ACM,* Vol. 15, Sept. 1972, pp. 820-826.

[6]Bryson, A. E. Jr. and Ho, Y. C., *Applied Optimal Control,* John Wiley and Sons, New York, 1975.

[7]Schaechter, D. B., "Estimation of Distributed Parameter Systems," *Journal of Guidance, Control and Dynamics,* Vol. 5, Jan./Feb. 1982, pp. 22-26.

[8]Eldred, D. B. and Schaechter, D. B., "Hardware Verification of Distributed/Adaptive Control," *Proceedings of the NASA/JPL Workshop on Applications of Distributed System Theory to the Control of Large Space Structures,* July 1982, Jet Propulsion Laboratory, Pasadena, Calif., Pub. 83-46, July 1983, pp. 337-350.

[9]Schaechter, D. B., "Adaptive Control for Large Space Structures," *Proceedings of the AIAA Guidance and Control Conference,* Gatlinburg, Tenn., Aug. 1983, pp. 606-611.